Influence of microphysics on the scaling of precipitation extremes with temperature

Martin S. Singh & Paul A. O'Gorman

S1 Details of microphysics schemes

Here we describe in further detail the different microphysics schemes used in this study.

Lin-hail

The Lin-hail microphysics scheme is based on *Lin et al.* (1983) as modified by the Goddard Cumulus Ensemble Modeling Group (*Tao and Simpson*, 1993; *Braun and Tao*, 2000). It includes six classes of water species representing water vapor, cloud water, cloud ice, rain, snow and hail. The size distributions of the precipitating species (rain, snow and hail) are assumed to follow an exponential distribution such that the concentration of particles of species i with diameter D_i per unit size interval is given by

$$n(D_i) = n_{0i} \exp\left(-\lambda_i D_i\right). \tag{S1}$$

Here n_{0i} is the intercept parameter and λ_i is the slope parameter, defined by

$$\lambda_r = \left(\frac{\pi \rho_r n_{0r}}{\rho_a r_r}\right)^{\frac{1}{4}},$$
$$\lambda_s = \left(\frac{\pi \rho_r n_{0s}}{\rho_a r_s}\right)^{\frac{1}{4}},$$
$$\lambda_h = \left(\frac{\pi \rho_h n_{0h}}{\rho_a r_h}\right)^{\frac{1}{4}},$$

where ρ is the density, r is the mixing ratio and the subscripts refer to dry air (a), rain (r), snow (s) and hail (h). Following *Potter* (1991), the density of liquid water ρ_r is used rather than the density of snow when calculating λ_s. Some of the values of the particle densities and intercept parameters differ from those used originally by *Lin et al.* (1983) and are given in table S1.

Based on the size distributions given above and an assumed form for the fall speed of each particle, the mass-weighted fall speeds of each hydrometeor species U_i may be written,

$$U_r = \frac{a_r \Gamma(4 + b_r)}{6 \lambda_r^{b_r}} \left(\frac{\rho_0}{\rho_a}\right)^{\frac{1}{2}},$$
$$U_s = \frac{a_s \Gamma(4 + b_s)}{6 \lambda_s^{b_s}} \left(\frac{\rho_0}{\rho_a}\right)^{\frac{1}{2}},$$
$$U_h = \frac{\Gamma(4.5)}{6 \lambda_h^{\frac{1}{2}}} \left(\frac{4 g \rho_h}{3 C_D \rho_a}\right)^{\frac{1}{2}}.$$

Here, $\Gamma(\cdot)$ is the gamma function, ρ_0 is the dry air density at the surface, and the constants are defined in table S1. The microphysical source and sink terms of each water species are calculated following *Lin et al.* (1983) as modified by *Braun and Tao* (2000), and a saturation adjustment similar to *Tao et al.* (1989) is applied to prevent supersaturation. Cloud water is assumed to have zero fall speed relative to air, while cloud ice is assumed to fall at a uniform velocity of 0.2 m s^{-1}.

Lin-graupel

The Lin-graupel scheme is similar to the Lin-hail scheme, except that it includes graupel as one of the frozen hydrometeor species instead of hail. The size distribution of graupel is defined by (S1), but it is assumed to have a smaller density, ρ_g, and a larger intercept parameter, n_{0g}, compared to that of hail (table S1) and a different form for the mass-weighted fall speed given by (*Rutledge and Hobbs*, 1984),

$$U_g = \frac{a_g \Gamma(4 + b_g)}{6\lambda_g^{b_g}} \left(\frac{\rho_0}{\rho}\right)^{\frac{1}{2}}, \tag{S2}$$

where the slope parameter for graupel is defined,

$$\lambda_g = \left(\frac{\pi \rho_g n_{0g}}{\rho_a r_g}\right)^{\frac{1}{4}}.$$

The functional form of the microphysical source and sink terms for graupel are identical to those of hail in the Lin-hail scheme, but, because of the different density, intercept parameter and fall speed of graupel, the magnitude of these tendency terms differ, even for identical environmental conditions.

Fixed-fall speed

The fixed-fall speed simulations described in section 5 use an altered form of the Lin-hail scheme in which the fall speed of all hydrometeors are fixed to given values for the purposes of the precipitation fallout calculation. However, the fall speed of cloud ice remains set to 0.2 m s^{-1}, and the microphysical source and sink terms are calculated based on the fall speeds as given by the original Lin-hail scheme.

Thompson

The microphysics scheme referred to as the Thompson scheme in this study is based on that of *Thompson et al.* (2008). As with the Lin-based schemes, it includes six water species (vapor, cloud water, cloud ice, rain, snow and graupel). However, unlike the Lin-based schemes, the Thompson scheme assumes the size distributions of all hydrometeors except snow follow a generalized gamma distribution, and it includes as prognostic variables the number concentration of cloud ice particles and rain drops in addition to the mixing ratio of each water species. Thus, the Thompson scheme is a two-moment scheme for cloud ice and rain water, and a one-moment scheme for all other condensate species[1]. In addition, *Thompson et al.* (2008) allows for the distribution parameters of the hydrometeor species to depend on their mixing ratio in an attempt to emulate the behavior of more comprehensive, fully two-moment schemes (e.g., *Morrison et al.*, 2005). In the simulations used in this study, we assume a fixed number concentration of cloud droplets characteristic of maritime conditions of 100 cm^{-3}.

S2 Condensation extremes in RCE

Here we analyze the scaling of instantaneous net-condensation extremes[2] in the simulations in further detail. We consider a decomposition of the net condensation similar to the scaling used by *Muller et al.* (2011):

$$C_e = -\epsilon_C \int_0^{z_t} \frac{\partial \overline{q^*}}{\partial z} \overline{\rho} w_e \, dz. \tag{S3}$$

[1] In *Thompson et al.* (2008) only cloud ice is treated as two-moment, but in the implementation used in this study rain is also included as a two-moment species.

[2] Considering condensation rather than net condensation (i.e., neglecting the contribution of grid boxes in which the microphysical tendency of water vapor is positive) results in values of condensation extremes that differ by less than three percent.

Table S1: Parameters used in the Lin-hail and Lin-graupel microphysics schemes.

Symbol	Description	Value	Units
n_{0r}	Intercept parameter for rain	8×10^6	m^{-4}
ρ_r	Density of rain water	1000	kg m^{-3}
a_r	Rain fall speed constant	842	m^{1-b_r} s^{-1}
b_r	Rain fall speed exponent	0.8	
n_{0s}	Intercept parameter for snow	1×10^8	m^{-4}
a_s	Snow fall speed constant	12.4	m^{1-b_s} s^{-1}
b_s	Snow fall speed exponent	0.42	
n_{0h}	Intercept parameter for hail	2×10^4	m^{-4}
ρ_h	Density of hail stones	900	kg m^{-3}
C_D	Drag co-efficient	0.6	
n_{0g}	Intercept parameter for graupel	4×10^6	m^{-4}
ρ_g	Density of graupel particles	400	kg m^{-3}
a_g	Graupel fall speed constant	19.3	m^{1-b_g} s^{-1}
b_g	Graupel fall speed exponent	0.37	

Here C_e is the 99.99th percentile of column net condensation, ρ is the air density, q^* is the saturation specific humidity, the over-bar represents a time and domain mean and z_t is the height of the tropopause (taken to be the level at which the lapse rate equals 2 K km^{-1}). The vertical velocity profile $w_e(z)$ is calculated as the mean vertical velocity for points at which the column net-condensation rate exceeds its 99.99th percentile. The integral in (S3) represents an estimate of the column net-condensation rate derived from the dry static energy budget (see *Muller et al.*, 2011). The derivation neglects storage, horizontal advection and deviations from moist adiabatic lapse rates; the inaccuracies in the estimate associated with these approximations are collected into the condensation efficiency ϵ_C so that (S3) is exactly satisfied.

According to (S3), for a simple mass-flux profile with convergence near the surface and divergence near the tropopause, net-condensation extremes follow CC scaling if the mass-flux profile and the efficiency ϵ_C are invariant under warming. Deviations of net-condensation extremes from CC scaling result from a more realistic mass-flux profile, or from changes in the mass-flux profile or condensation efficiency with temperature. As discussed in *Muller et al.* (2011), the expression for the condensation rate (S3) includes the vertical velocity within an integral weighted by the vertical gradient in saturation specific humidity. This vertical gradient maximizes at the surface and decreases exponentially above, which gives the low-level vertical velocity more weight in determining the condensation rate compared to the vertical velocity at higher levels. As pointed out in section 4, the negative low-level changes in w_e are thus an important negative influence on net-condensation extremes in our simulations.

In the Lin-hail simulations, the condensation efficiency ϵ_C decreases between 0.84 and 0.75 across the intermediate-resolution simulations (Fig. S4), with the condensation efficiency behaving similarly for simulations with the other microphysics schemes. However, the changes in ϵ_C depend on the precise form of (S3) used. *Muller* (2013), used a slightly different approach in which the net-condensation rate was estimated based on the vertical gradient of dry static energy rather than saturation specific humidity. With this approach, the condensation efficiency ϵ_C does not decrease monotonically with warming in the Lin-hail simulations. Regardless of the precise form of (S3) used, however, the fractional changes in ϵ_C with warming are generally considerably smaller than fractional changes in the precipitation efficiency ϵ_P defined in section 5.

References

Braun, S. A., and W.-K. Tao (2000), Sensitivity of high-resolution simulations of hurricane Bob (1991) to planetary boundary layer parameterizations, *Mon. Wea. Rev.*, *128*, 3941–3961.

Lin, Y.-L., R. D. Farley, and H. D. Orville (1983), Bulk parameterization of the snow field in a cloud model, *J. Clim. Appl. Meteorol.*, *22*, 1065–1092.

Morrison, H., J. A. Curry, and V. I. Khvorostyanov (2005), A new double-moment microphysics parameterization for application in cloud and climate models. Part I: Description, *J. Atm. Sci.*, *62*, 1665–1677.

Muller, C. (2013), Impact of convective organization on the response of tropical precipitation extremes to warming, *J. Climate*, *26*, 5028–5043.

Muller, C. J., P. A. O'Gorman, and L. E. Back (2011), Intensification of precipitation extremes with warming in a cloud-resolving model, *J. Climate*, *24*, 2784–2800.

Potter, B. E. (1991), Improvements to a commonly used cloud microphysical bulk parameterization, *J. Appl. Meteorol.*, *30*, 1040–1042.

Rutledge, S. A., and P. V. Hobbs (1984), The mesoscale and microscale structure and organization of clouds and precipitation in midlatitude cyclones. XII: A diagnostic modeling study of precipitation development in narrow cold-frontal rainbands, *J. Atm. Sci.*, *41*, 2949–2972.

Tao, W.-K., and J. Simpson (1993), The Goddard cumulus ensemble model. Part I: Model description, *Terr. Atmos. Oceanic Sci.*, *4*, 35–72.

Tao, W.-K., J. Simpson, and M. McCumber (1989), An ice-water saturation adjustment, *Mon. Wea. Rev.*, *117*, 231–235.

Thompson, G., P. R. Field, R. M. Rasmussen, and W. D. Hall (2008), Explicit forecasts of winter precipitation using an improved bulk microphysics scheme. Part II: Implementation of a new snow parameterization, *Mon. Wea. Rev.*, *136*, 5095–5115.

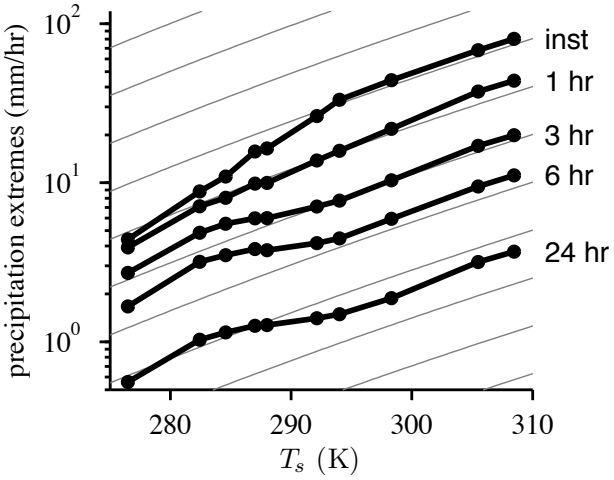

Figure S1: As in Fig. 2 but for high-resolution simulations using the Lin-hail microphysics scheme. The larger sample size at this resolution allows daily accumulations (24 hr) to be also included.

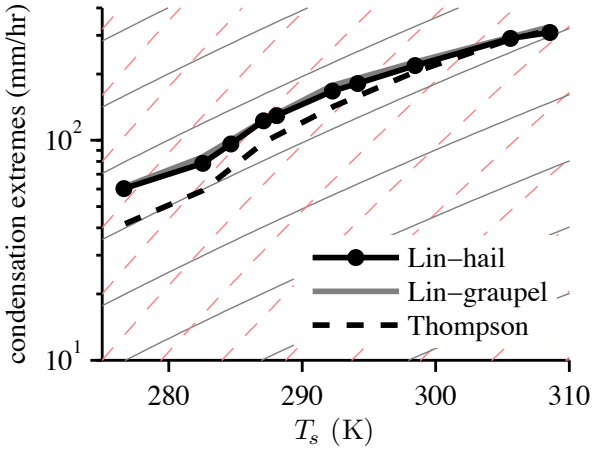

Figure S2: The 99.99th percentile of instantaneous column net-condensation rate as a function of the mean temperature of the lowest model level (T_s). Simulations with Lin-hail (black), Lin-graupel (thick-gray) and Thompson (dashed) microphysics schemes are shown. Thin gray lines are contours proportional to the surface saturation specific humidity, and red-dashed lines are proportional to the square of the surface saturation specific humidity; each successive line corresponds to a factor of two increase.

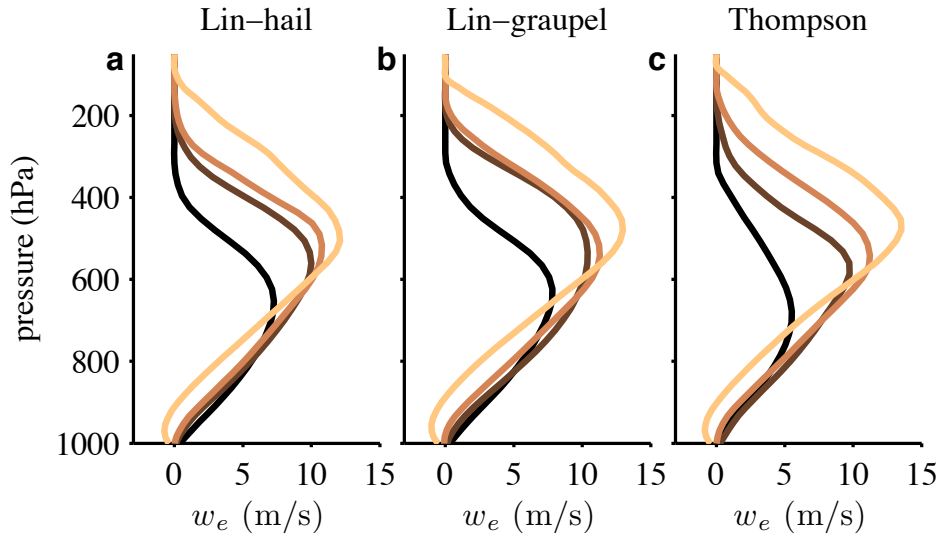

Figure S3: Mean vertical velocity profiles for columns in which the instantaneous column net-condensation rate exceeds its 99.99th percentile. (a) Lin-hail simulations with mean temperatures of the lowest model level (T_s) of 277 (black), 292, 298 and 309 K (orange). (b) Lin-graupel simulations with T_s equal to 277 (black), 292, 298 and 308 K (orange). (c) Thompson simulations with T_s equal to 277 (black), 292, 298 and 308 K (orange).

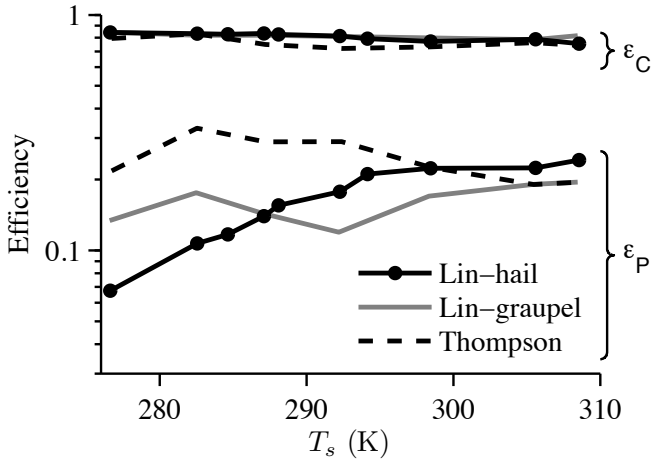

Figure S4: Condensation efficiencies [ϵ_C; defined in (S3)] and precipitation efficiencies [ϵ_P; defined in (1)] as a function of the mean temperature of the lowest model level (T_s). Results for simulations using the Lin-hail (black), Lin-graupel (gray) and Thompson (dashed) microphysics schemes are shown.

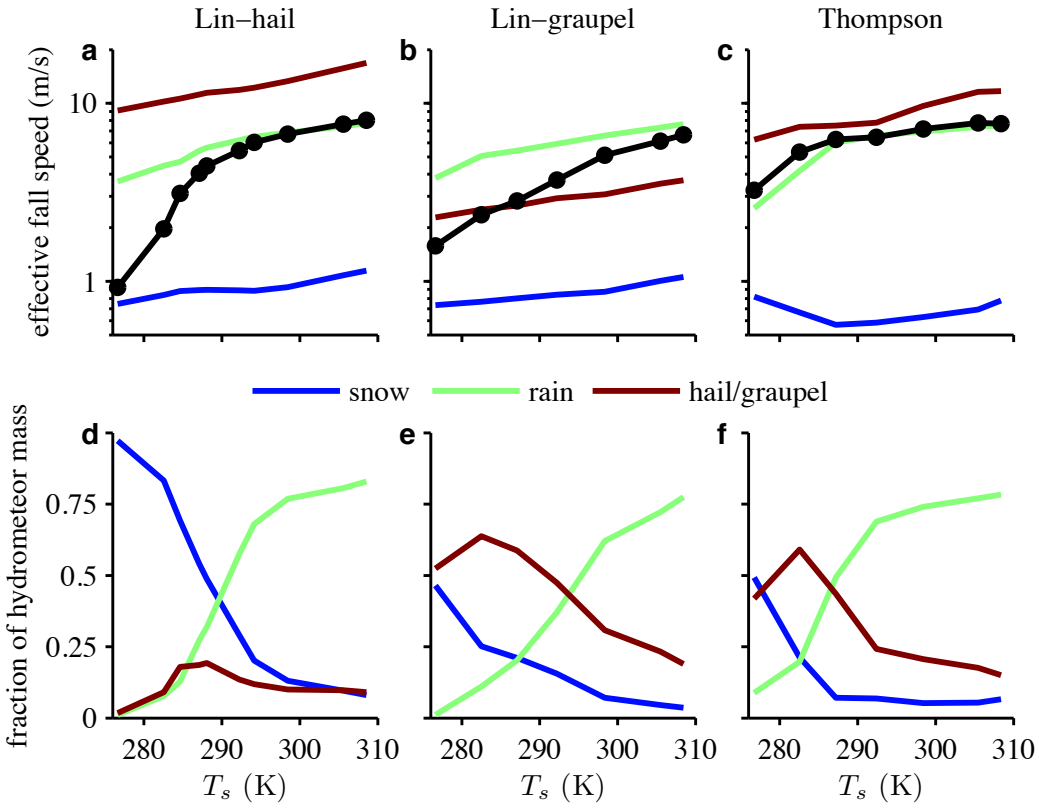

Figure S5: (a,b,c) Effective hydrometeor fall speed, v_f (black), and effective fall speed of snow (blue), rain (green) and hail/graupel (maroon) defined analogously to v_f but only considering the specific hydrometeor. (d,e,f) Fraction of total column hydrometeor mass comprised of each hydrometeor species for columns in which the instantaneous precipitation rate exceeds its 99.99th percentile [colors same as in (a)]. Lin-hail (left), Lin-graupel (center) and Thompson (right) simulations are shown.